Adaptive simplification of complex multiscale systems

Eliodoro Chiavazzo[1,*] and Ilya Karlin[2,3,†]

[1]*Department of Energetics, Politecnico di Torino, 10129 Torino, Italy*
[2]*Aerothermochemistry and Combustion Systems Lab, ETH Zurich, CH-8092 Zurich, Switzerland*
[3]*School of Engineering Sciences, University of Southampton, SO17 1BJ Southampton, United Kingdom*

A fully adaptive methodology is developed for reducing the complexity of large dissipative systems. This represents a significant step toward extracting essential physical knowledge from complex systems, by addressing the challenging problem of a minimal number of variables needed to exactly capture the system dynamics. Accurate reduced description is achieved, by construction of a hierarchy of slow invariant manifolds, with an embarrassingly simple implementation in any dimension. The method is validated with the autoignition of the hydrogen-air mixture where a reduction to a cascade of slow invariant manifolds is observed.

I. INTRODUCTION

Detailed reaction mechanisms typically serve as accurate models of dissipative complex systems with many interacting components: Biochemical processes in living cells and combustion phenomena are prototypical examples of such systems [1–3]. Modern research has to cope with an increasing complexity mainly in two aspects: First, the number of degrees of freedom (scaling with the number of components) is tremendously large; second, complex system dynamics is characterized by a wide range of time scales. For example, the usage of detailed reaction mechanisms in the reactive flow simulation soon becomes intractable even for supercomputers, particularly in the turbulent combustion of even "simplest" fuels such as hydrogen [4–6]. As a result, there is a strong demand for methodologies capable of both drastically reducing the description of complex systems with a large number of variables, and concurrently allowing physical insights to be gained. Modern automated approaches to model reduction are based on the notion of low-dimensional manifold of the slow motions [slow invariant manifold (SIM)] in the phase space describing the asymptotic system behavior. Although several methodologies have been suggested in the literature [7], the construction of an accurate reduced description remains a rather challenging task. In particular, the evaluation of numerical SIM approximations in the phase space is hindered by several difficulties as far as the choice of the manifold dimension is concerned, because the latter information is typically not known *a priori*. In addition, accurate simplification of complex multiscale systems often requires the construction of heterogeneous (variable dimension) manifolds with the dimension d ranging from unity up to tens in different regions of the phase space. To the best of our knowledge, at the present, fully adaptive model reduction methodologies capable of coping with the above issues are still missing. This research area is fairly active and much effort has been devoted to devising techniques with the above features. The intrinsic low-dimensional manifold (ILDM) approach [8], the computational singular perturbation (CSP) method [9], and

the minimal entropy production trajectory (MEPT) method [10] are only some representative examples. In addition, the minimal number of reduced degrees of freedom underling the asymptotic dynamics of complex multiscale systems is still a debated issue [11]. In this respect, we notice that, although here we mainly focus on chemical kinetics, our results have direct implications on the study of the homogeneous isotropic Boltzmann equation that has been stated as a fundamental problem of physics [12]. The latter investigation is beyond the scope of this work, however, future studies shall move in this direction, where we can take advantage of recently introduced models such as the one proposed in Ref. [13].

In the present work, we introduce a methodology that enables to cope with the accurate reduced description of large dissipative systems, where no *a priori* assumptions on the least number of fundamental (slow) variables are made. Toward this end, both global and local construction of slow invariant manifolds, with an embarrassingly simple implementation up to any dimension, is worked out.

This paper is organized in sections as follows. In Sec. II, we briefly review the governing equations for chemical kinetics. The problem of model reduction, as understood by the method of invariant manifold (MIM), is discussed in Sec. III. The relaxation redistribution method (RRM) is introduced in Sec. IV, where both a global (Sec. IV A) and a local (Sec. IV A) formulation are presented. The latter methodology is validated for a detailed chemical kinetics describing a reacting mixture of hydrogen and air in Sec. V. Finally, conclusions are drawn in Sec. VI.

II. DISSIPATIVE REACTION KINETICS

In the present study, we assume that a complex dissipative dynamics is governed by an autonomous system in terms of the state ψ on a phase space U with a unique steady state,

$$\frac{d\psi}{dt} = f(\psi). \tag{1}$$

An important example of (1) to be addressed below is the reaction kinetics, where $\psi = (\psi_1, \ldots, \psi_n)$ is a n-dimensional vector of concentrations of various species, while the vector field f is constructed according to a detailed reaction mechanism as described below. More specifically, in a closed

*eliodoro.chiavazzo@polito.it
†karlin@lav.mavt.ethz.ch

reactive system, the complex reaction of n chemical species $A_1, \ldots, A_n$ and d elements can be represented by a (typically) large number r of elementary steps:

$$\sum_{i=1}^{n} \alpha_{si} A_i \rightleftarrows \sum_{i=1}^{n} \beta_{si} A_i, \quad s = 1, \ldots, r, \qquad (2)$$
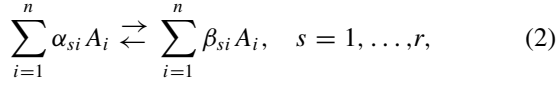
where α_{si} and β_{si} are the stoichiometric coefficients. The latter coefficients enable to define the three stoichiometric vectors: $\alpha_s = (\alpha_{s1}, \ldots, \alpha_{sn})$, $\beta_s = (\beta_{s1}, \ldots, \beta_{sn})$, and $\gamma_s = \beta_s - \alpha_s$, where the index s runs over the r elementary reactions (2). For clarity, in the detailed reaction mechanism for air and hydrogen to be considered below [3], s identifies any of the 21 reactions in Table I, while the corresponding stoichiometric coefficients α_{si} and β_{si} indicate the number of molecules of species i in the reactants and products of reaction s, respectively. Production (or depletion) rates of chemical species can be conveniently expressed in terms of the differences: $\gamma_{si} = \beta_{si} - \alpha_{si}$.

Expressing the state in terms of the molar concentrations $\psi = (c_1, \ldots, c_n)$ (ratios of the number of moles by the volume), all chemical species evolve in time according to the mechanism (2):

$$\frac{d\psi}{dt} = \sum_{s=1}^{r} \gamma_s W_s(\psi, \theta), \qquad (3)$$

where $W_s(\psi)$ is the reaction rate function of the reaction s, which (usually) takes a polynomial form according to the mass action law,

$$\begin{aligned} W_s(\psi) &= W_s^+(\psi, \theta) - W_s^-(\psi, \theta) \\ &= k_s^+(\theta) \prod_{i=1}^{n} c_i^{\alpha_i} - k_s^-(\theta) \prod_{i=1}^{n} c_i^{\beta_i}, \end{aligned} \qquad (4)$$

with the reaction constants k_s^+ and k_s^- depending on the system temperature θ according to the Arrhenius equation,

$$k_s(\theta) = A_s \theta^{n_s} e^{-E_{as}/\mathcal{R}\theta}, \qquad (5)$$

where the quantities A_s, n_s, E_{as} are fixed (and tabulated, see, e.g., Table I) and referred to as preexponential factor, temperature exponent, and activation energy of the reaction s, respectively, while $\mathcal{R}$ is the universal gas constant. Owing to the principle of detailed balance, a relationship between the latter reaction constants (k_s^+, k_s^-) is established for each step s at the steady state: $W_s^+ = W_s^-$. In general, the system (3) is to be solved in combination with an additional equation ruling the temperature evolution (energy equation).

The concentration of the ith chemical species can be also expressed in terms of the mass fraction $Y_i = \omega_i c_i / \bar{\rho}$, while, in an adiabatic closed system, the temperature is computed by conserving the mixture-averaged enthalpy, which for ideal gases reads

$$\bar{h} = \sum_{i=1}^{n} Y_i h_i(\theta), \qquad (6)$$

where $\bar{\rho}$, ω_i, and h_i are the mixture density, the molecular weight, and specific enthalpy (per unit mass) of species i, respectively. For the sake of completeness, we report here the closed dynamical system governing closed reactive ideal

mixtures under fixed enthalpy $\bar{h}$ and pressure p, to be addressed below in Sec. V:

$$\begin{cases} d\psi/dt = \sum_{s=1}^{r} \gamma_s W_s(\psi, \theta) = (dc_1/dt, \ldots, dc_n/dt), \\ d\theta/dt = -\frac{1}{\bar{C}_p} \sum_{i=1}^{n} h_i(\theta) \dot{Y}_i, \end{cases} \qquad (7)$$

where $\bar{C}_p$ denotes the mixture-averaged specific heat under fixed pressure, while specific enthalpy $h_i(\theta)$ for any species i can be computed using (10). Molar concentrations c_i are linked to mass fractions Y_i as $c_i = p(Y_i/\omega_i)/(\mathcal{R}\theta \sum_j^n Y_j/\omega_j)$, while the mass fraction rate $\dot{Y}_i$ reads as follows: $\dot{Y}_i = \omega_i \bar{\rho}^{-1} dc_i/dt$, where ω_i is the molecular weight of species i. We notice that the second equation in (7) stipulates the conservation of $\bar{h}$, thus it represents an alternative way of imposing constance of (6).

Finally, owing to the conservation of elements, in a closed reactor, d linear combinations of the species concentrations (expressing the number of moles of each element) remain constant during the system evolution in time:

$$C\psi = \text{const}, \qquad (8)$$

where C is a $d \times n$ fixed matrix.

Remark: Having in mind dissipative multiscale dynamics such as chemical and physical kinetics, here we focus on systems (1) with a single steady state. Hence, the RRM introduced below in Sec. IV has been tested for those cases so far. We stress, however, that, for deriving the RRM approach, no assumptions are made concerning the number of steady-state points of (1). Thus, implementations of the RRM to different dynamics shall be presented in future publications.

A. Thermodynamic Lyapunov function

Owing to the second law of thermodynamics, the kinetic equations (3) are equipped with a global thermodynamic Lyapunov function $G(\psi)$. In other words, the time derivative of the above state function is nonpositive in the whole phase space, $\dot{G}(\psi) \leqslant 0$, with the equality holding at steady state. For instance, in an adiabatic reactor with fixed pressure p and enthalpy $\bar{h}$, the specific mixture-averaged entropy $\bar{s}$ (in mass units) monotonically increases in time starting from any nonequilibrium initial condition: Hence the function $G = -\bar{s}$ decreases during the dynamics. For an ideal gas mixtures, a Lyapunov function G of the system (3) takes the explicit form

$$G = -\bar{s} = -\sum_{i=1}^{n} X_i[s_i(\theta) - \mathcal{R} \ln X_i - \mathcal{R} \ln(p/p_{\text{ref}})]/\bar{W}, \quad (9)$$

where $X_i = c_i / \sum_{i=1}^{n} c_i$ and s_i denote the mole fraction and the specific entropy of species i, respectively, $\mathcal{R}$ is the universal gas constant, p_{ref} a reference pressure, and $\bar{W}$ the mean molecular weight. For numerical purposes, the properties of the ith species, h_i and s_i, can be expressed in terms of the temperature, θ, and a set of tabulated coefficients a_{ij} as

follows [14]:

$$h_i(\theta) = \mathcal{R}\theta\left(a_{i1} + \frac{a_{i2}}{2}\theta + \frac{a_{i3}}{3}\theta^2 + \frac{a_{i4}}{4}\theta^3 + \frac{a_{i5}}{5}\theta^4 + \frac{a_{i6}}{\theta}\right),$$

$$s_i(\theta) = \mathcal{R}\left(a_{1i}\ln\theta + a_{i2}\theta + \frac{a_{i3}}{2}\theta^2 + \frac{a_{i4}}{3}\theta^3 + \frac{a_{i5}}{4}\theta^4 + a_{i7}\right).$$

(10)

III. THE FILM EQUATION OF DYNAMICS

If the number of degrees of freedom n is large, one may seek a reduced description with a smaller number of variables $q \ll n$. A consistent approach to model reduction is provided by the MIM, whose brief review is in order. For further details, please see Ref. [15].

In MIM, the problem of model reduction is identified with the construction of a slow invariant manifold (SIM) Ω_{SIM}, whose dimension q is the number of the essential (macroscopic) variables that parametrize the SIM.

As sketched in Fig. 1(a), the above method is based on the idea that the macroscopic *slow* dynamics of a complex system occurs along the SIM (invariance), once an initial *fast* relaxation toward the SIM has taken place. Let a manifold Ω (not necessarily a SIM) be embedded in the phase space U and defined by a function $\Omega = \psi(\xi)$, which maps a macroscopic variables space Ξ into U. Introducing a projector P onto the tangent space T of a manifold Ω, the reduced dynamics on it is defined by the projection $Pf(\Omega) \in T$ [see Fig. 1(b)]. A manifold Ω is termed invariant (but not necessarily slow) if the vector field f is tangent to the manifold at every point: $f(\psi(\xi)) - Pf(\psi(\xi)) = 0, \xi \in \Xi$.

While the notion of a manifold's invariance is relatively straightforward, a definition of slowness is more delicate as it necessarily compares a (faster) approach toward the SIM with a (slower) motion along SIM. In MIM, slowness is understood as stability, and SIM is a stable stationary solution $\psi_{\text{SIM}}(\xi)$ of
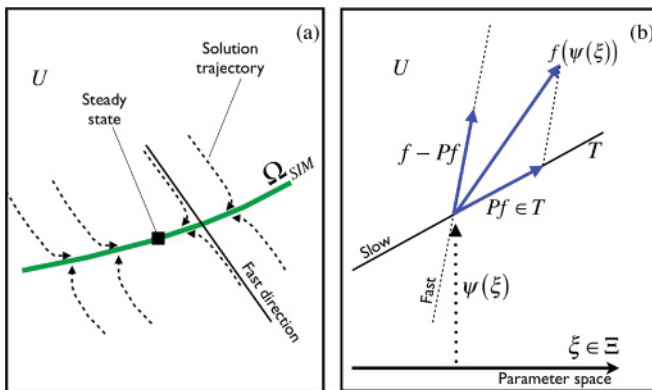

FIG. 1. (Color online) (a) Model reduction techniques assume the following idea: After a fast initial transient at the time instants $t \leqslant t_0$, the (slow) dynamics of a complex system takes place along a slow invariant manifold (SIM) on the phase space U at any future works $t > t_0$ (invariance) toward the steady state. (b) The definition of a projector P onto the tangent space T introduces a decomposition of slow and fast motions of the field f. In a vicinity of the SIM, slow and fast motions are locked in the image and null space of the thermodynamic projector P [15,16], respectively.
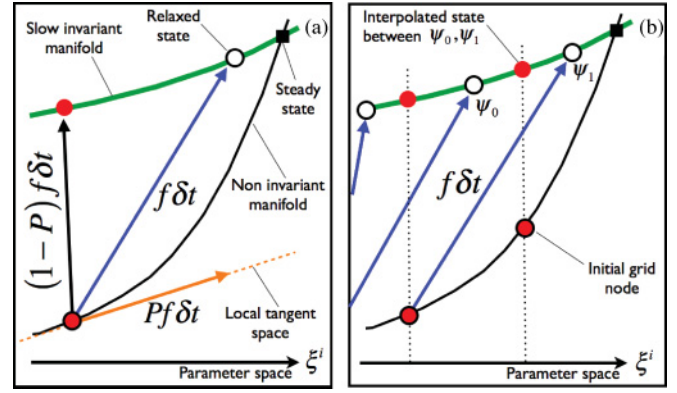

FIG. 2. (Color online) (a) The relaxation owing to (1) of a noninvariant manifold. Fast dynamics drives it toward the slow invariant manifold, whereas the concurrent action of the slow dynamics causes a shift toward the steady state (shagreen effect). On the contrary, relaxation owing to the film equations (11) and (12) allows movements only in the fast subspace. (b) RRM. The displacement in the slow subspace, generated during relaxation, is annihilated by a redistribution step in the parameter space.

the following film equation of dynamics defined on the space of maps $\psi(\xi)$ [15],

$$\frac{d\psi(\xi)}{dt} = f(\psi(\xi)) - Pf(\psi(\xi)).$$

(11)

Rigorous proofs of existence and uniqueness of SIM, by the film equation (11), were recently given for linear systems [17], while the rationale behind the (11) is explained by means of a sketch in Fig. 2(a). Here, it is worth stressing that the above (11) denotes a partial differential equation (PDE) whose unknown is a mapping $\psi(\xi)$ from a low-dimensional reduced space $\Xi, \xi \in \Xi$ (also referred to as parameter space in the following) into the phase space $U, \psi \in U$. Therefore, readers should not get confused between stable stationary solutions of (11) (defining SIM as a mapping from Ξ into U) and single stationary states (or equilibrium states) of (1), ψ^{ss} [which satisfy the condition $f(\psi^{\text{ss}}) = 0$].

For thermodynamically consistent systems (1) equipped with a potential G [thermodynamic Lyapunov function with respect to (1)], MIM offers a projector whose construction is based on the tangent space T and the gradient of the thermodynamic potential, $\partial G/\partial\psi$, at every point of SIM. This consistently imposes that the reduced dynamics $Pf(\psi(\xi))$ is dissipative. Explicit formulas for this thermodynamic projector are not necessary for the scope of this paper, and can be found in Ref. [15]. Importantly, separation of motions in a vicinity of SIM is dictated by thermodynamic projector P, because it can be proved that slow motions along SIM are locked in the image, $\text{im}P = T$, whereas the null space, $\ker P$, spans the fibers of fast motions transversal to SIM [Fig. 1(b)] [16].

Finally, a computationally advantageous realization is provided by a grid representation of MIM [18], where grid nodes in the phase space are defined by a discrete set of macroscopic variables, ξ, while finite-difference operators are used to compute the tangent space at every node $\psi(\xi)$. Thanks to locality of MIM constructions, we further make no distinction between manifolds and grids.

Remark: Consistent constructive methods of slow invariant manifolds rely upon efficient methods for solving the PDE (11). As discussed below in Sec. III A, toward this aim, finite-difference schemes have been suggested in the literature [15,19,20] [see also (12)]. Nevertheless, to the best of our knowledge, only explicit (or semi-implicit) schemes are available so far. Thus, owing to hyperbolicity of Eq. (11), its numerical solution is hindered by numerical instabilities (i.e., Courant type) [19], and no satisfactory solution to this issue has been suggested up to now. It is useful to stress that here we review the notion of film equation only for a better understanding of the present work. In fact, our suggestion toward the effective answer to the above problem is to avoid a direct solution of (11) (e.g., by finite-difference schemes) in favor of its emulation, where the problematic term $-Pf$ is not approximated with finite differences but mimicked by a redistribution step in terms of macroscopic variables (see Sec. IV below).

A. Direct solution of the film equation

A natural approach to the construction of SIMs is a direct numerical solution of the film equation (11) starting with an initial (usually noninvariant) manifold. For that, both the initial condition as well as implicit or semi-implicit schemes were developed. The simplest explicit scheme for solving Eq. (11) can be realized by iteratively refining each point ψ of the initial manifold, $\psi + d\psi$,

$$d\psi = \tau(f(\psi) - Pf(\psi)), \qquad (12)$$

with the time τ being estimated according to the suggestions in Ref. [18], where the scheme (12) is referred to as the relaxation method. It has been noticed [19] that the solution of the film equation of dynamics (11), similarly to hyperbolic partial differential equations for computational fluid dynamics (CFD) simulations, is hindered by severe numerical instabilities (see, e.g., the Courant instability [21]). Furthermore, we notice that, unlike CFD, the numerical solution of (11) comes with additional difficulties, owing to an uncontrolled variation of the grid-node spacing. As a result, it is difficult to formulate an analog of the Courant-Friedrichs-Lewy (CFL) condition [21] for (12), and the suppression of instability was only attempted by an arbitrary decrease of the time τ until convergence [19]. In general, the latter approach proves rather poor because the lack of convergence of (12) might not have a numerical origin. In fact, there is no guarantee that the chosen number of reduced degrees of freedom q reveals is sufficient in describing the asymptotic behavior of the dynamical system (1) in a given domain of the phase space. For instance, in the case where a higher number of reduced variables are requested, the refinement of a q-dimensional manifold by stable numerical schemes of (11) is expected to fail anyway. The idea of an adaptive dimension of SIM, formulated below in Sec. IV B, is based on the latter observation.

Finally, the construction of slow invariant manifolds by the solution of (11) has been always attempted in the whole phase space, by assigning *a priori* their dimension q somewhat arbitrarily. Such an approach, where the dimension q comes as an external input into the problem, poses severe limitations to the accuracy of the reduced description and, most detrimentally, hinders the gaining of any better physical knowledge about it.

Moreover, construction of high-dimensional invariant manifolds ($q \geqslant 3$) by (11) is quite problematic and, to the best of our knowledge, was never successfully accomplished up to now.

IV. THE RELAXATION REDISTRIBUTION METHOD

Toward the end of overcoming the above drawbacks, in this work, we introduce an approach to model reduction, which allows for the construction of slow invariant manifolds with the dimension q adaptively varying from one region of the phase space to another. We address thereby the fundamental issue of the minimal number of important (slow) variables that underlie the behavior of a complex dissipative phenomenon in a region of the phase space: A knowledge, emerging from the system and no longer imposed, is now gained. The latter is a challenging problem in physics, and even in the classical cases, such as the reduced description of the Boltzmann kinetic equation by a finite set of velocity moments of the distribution function (see, e.g., Ref. [22]), some essential questions remain open [11,23, 24]. Similarly, in chemical kinetics, several methods have been suggested [25–27] for approximating and parametrizing the SIM—however, the choice of the minimal number of chemical coordinates (manifold parameters) is still debated.

In the following, the key idea of our approach is to abandon an attempt of solving the film equation (11) by numerical schemes such as (12), in favor of a simulation of the physics behind this equation, in a spirit similar to the Monte Carlo methods: As a consequence, a highly efficient construction of SIM with an embarrassingly simple implementation in any dimension is derived.

A. Global formulation of RRM

In order to introduce our method, we consider reaction kinetics and assume that a slow dynamics of (1) evolves on a q-dimensional SIM in the n-dimensional concentration space (this assumption will be relaxed in a sequel). Inspection of the right-hand side of (11) reveals a composition of two motions: The first term, $f(\psi(\xi))$, is the relaxation of the initial approximation to SIM owing to the detailed kinetics, while the second term, $-Pf(\psi(\xi))$ is the motion antiparallel to the slow dynamics. Let a time stepping δt and a numerical scheme (e.g., Euler, Runge-Kutta, etc.) be chosen for solving the system of kinetic equations: All grid nodes relax toward the SIM under the full dynamics f during δt. The fast component of f leads any grid node closer to the SIM while, at the same time, the slow component causes a shift toward the steady state [see Fig. 2(a)]. As a result, while continuing to relax, the grid shrinks toward the steady state (we term this a "shagreen effect" per de Balzac's famous novel [28]—chagrin in French). Subtraction of the slow component therefore prevents the shagreen effect from occurring, and it is precisely the difficulty in the numerical realization: Explicit evaluation of the projector P on the approximate SIM does not always balance the effect of shrinking. This leads to instabilities, and results in a drastic decreasing of the time step.

The key idea here is to neutralize the slow component of motion by a redistribution of the points on the manifold after the relaxation step [see Fig. 2(b)]. For the sake of presentation, we assume that macroscopic parameters are given by a set of q linear functions $b = \{b_1, \ldots, b_q\}$ such that $b_1(\psi) = \xi^1, \ldots,$

$b_q(\psi) = \xi^q$. Let $\xi = (\xi^1, \ldots, \xi^q)$ be a generic node of a fixed grid S in the parameter space Ξ, and the q-dimensional slow invariant grid (SIG) in the phase space U is initialized: $\Omega^{in} = \psi^{in}(\xi)$ [that is, the initial SIG is the collection of nodes $\psi^{in} = \psi^{in}(\xi)$, $\xi \in S$]. After the relaxation step, all the nodes ψ^{in} have moved to new locations, $\psi^{in} \to \psi^R$, and we denote $\xi^R = b(\psi^R)$ the values of the macroscopic parameters corresponding to the relaxed nodes ψ^R.

It is worth stressing that by parameter space here we mean the low-dimensional macroscopic space Ξ whose dimension is $q \ll n$. Hence, an arbitrary grid S is defined by a mapping, $\psi(\xi)$, on a subspace of Ξ into the phase space U (of dimension n).

For example, the forward Euler scheme used below gives

$$\psi^R = \psi^{in}(\xi) + \delta t f(\psi^{in}(\xi)). \tag{13}$$

With this, also the nodes of the grid S shift by an amount $\delta\xi = b(\psi^R) - \xi$ owing to the slow component of motion. The redistribution of the nodes ψ^R back to the fixed grid S simulates the subtraction of the slow motion from the relaxation step, and is done as follows: For each $\xi \in S$, we consider a q-simplex S_q (in U) with $q + 1$ vertices $\psi_0^R, \psi_1^R, \ldots, \psi_q^R$ such that ξ is inside the macroscopic projection of S_q, the simplex Σ_q (in Ξ) formed by the vertices $\xi_0^R = b(\psi_0^R)$, $\xi_1^R = b(\psi_1^R)$, $\ldots$, $\xi_q^R = b(\psi_q^R)$. The updated (relaxed-and-redistributed) grid Ω^{RR} is constructed by a linear interpolation of the vertices of the simplex S_q:

$$\psi^{RR} = \left(1 - \sum_{i=1}^q w_i\right)\psi_0^R + \sum_{i=1}^q w_i \psi_i^R, \tag{14}$$

where the weights w_i are so chosen as to satisfy the redistribution condition,

$$b(\psi^{RR}) = \xi. \tag{15}$$

This amounts to solving a $q \times q$ linear system,

$$\sum_{j=1}^q \left[b_j(\psi_i^R) - b_j(\psi_0^R) \right] w_j = \xi^i - b_i(\psi_0^R). \tag{16}$$

The above procedure is supplemented by the boundary conditions applied at the edges of the grid: Grid nodes at the boundary ψ_b are reconstructed by extrapolation after the relaxation step. Formula (14) is used where $\psi^{RR} = \psi_b \notin S_q$ is located in the vicinity of a simplex S_q with vertices $\psi_0^R, \psi_1^R, \ldots, \psi_q^R$. In general, S_q can be chosen in such a way that its vertices are the relaxed states of the initial nodes $\psi_0^{in}, \psi_1^{in}, \ldots, \psi_q^{in}$ with $\psi_b = \psi_0^{in}$.

Thus, after the redistribution step, the initial grid is refined toward the invariant grid. The procedure is then iterated, whereas each relaxation step is altered by the redistribution step, in which the slow motion is subtracted by stretching the macroscopic variables to the nodes of the initial grid S.

We notice that, on SIM, movements owing to the vector field f occur along the manifold itself, thus the effect of the relaxation is entirely counterbalanced by the subsequent redistribution on the SIM. It is worth stressing that this observation holds for every invariant manifold (not necessarily SIM). Nevertheless, numerical evidences clearly show that an arbitrary invariant manifold Ω_{inv} is an unstable solution

of the above dynamics, and refinements starting from Ω_{inv} converge toward the SIM, which instead turns out to be a stable solution. As a result, slow invariant grids are stable stationary solutions of the described procedure, here termed RRM. Once the invariant grid is constructed, the reduced dynamics for variables ξ is defined as

$$\frac{d\xi}{dt} = b(f(\psi^{RR}(\xi))). \tag{17}$$

In other words, the suggested RRM enables to provide the reduced system (17), written in terms of a significantly smaller set of variables ξ, with a closure.

Note that, upon the global construction of SIG, computations deliver a discrete set of linked states $\psi^{RR}(\xi)$, in a vicinity of the corresponding slow invariant manifold. Here, grid nodes are termed "linked" because we assume that for any arbitrary node it is possible to identify all its nearest neighbors. Moreover, interconnectivity enables one to easily proceed with analytical continuation of the above slow invariant grid, and thus to the calculation of the right-hand side of (17) for any set of variables ξ. To this end, for simplicity, here we adopt multilinear interpolation, which possesses the advantage to automatically fulfill the linear conservation constraints (8). For further details on multilinear interpolation of grids, see Ref. [29]. On the other hand, if the local construction of SIG is implemented, a closure for (17) is computed when needed and no analytical continuation of the grid is requested. In the latter case, in order to speed up the computations, smart methodologies for data storage and retrieval can be used and are readily available from the literature [see, e.g., the *in situ* adaptive tabulation (ISAT) method in Ref. [30]].

Finally, note that while the redistribution step seems "natural" from the numerical standpoint of discretizing the above macroscopic equation (17) on a fixed grid S, the feature recognized here is that it is precisely the subtraction of the slow component of the motion in the film equation (11), which circumvents the question about explicit evaluation of slow motions in the course of the SIM construction.

In order to test the RRM, we first consider a simple benchmark suggested by Davis and Skodje (DS) [31] (a two-dimensional system with a one-dimensional SIM known in a closed analytical form). The DS system [31] consists of two equations,

$$\begin{aligned} dx/dt &= f_x(x) = -x, \\ dy/dt &= f_y(x,y) = -\gamma y + [(\gamma - 1)x + \gamma x^2]/(1 + x)^2, \\ \gamma &> 0, \end{aligned} \tag{18}$$

it has a unique stable steady state $x = y = 0$, and a one-dimensional SIM, $y = x/(1 + x)$. Here, when $\gamma \gg 1$, owing to a significant separation between of time scales of the two variables x and y, all solution trajectories of DS system exponentially decay to the SIM (see Ref. [31]). In the above notation, $\psi = (x, y)^T$, and we define the slow variable as $\xi = x$, that is, $b = (1, 0)$ and $b(\psi) = (1, 0)(x, y)^T = x$. The RRM is initialized with the grid represented by the collection of points $\{[x_r, y^{in}(x_r)]\}$, where x_r are distributed evenly in the interval $x \in [0, x_b]$. Upon the relaxation step, the grid points are shifted to new locations $\{[x_r, y^{in}(x_r)]\} \to \{[x_r^R, y^R(x_r)]\}$ with $x_r^R = (1 - \delta t)x_r$, $y_r^R = y^{in}(x_r) + \delta t f_y(x_r, y^{in}(x_r))$. Choosing
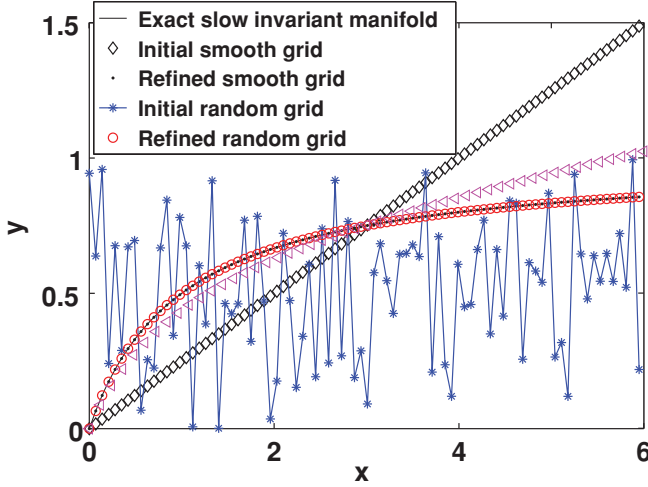
FIG. 3. (Color online) The Davis-Skodje system [31]. Two different initial grids are refined using the forward Euler scheme for the relaxation ($\delta t = 10^{-2}$). Results after 50 RRM iterations are reported (refined grids) with $\gamma = 50$. Triangles show an intermediate step (after two RRM iterations) starting from the initial smooth grid.

the interval $\Sigma_1 = [x_0^R, x_1^R]$ for each point x_r such that $x_r \in \Sigma_1$, the redistribution (14) gives

$$y_r^{RR} = \frac{(x_1^R - x_r)y_0^R + (x_r - x_0^R)y_1^R}{x_1^R - x_0^R}, \qquad (19)$$

while $x_r^{RR} = x_r$, by the condition (15). For the boundary node at x_b we set $y_0^R = y_b^R$ and for $y_1^R = y^R(x_{b-1})$, with $x_{b-1} \in S$ being the nearest neighbor of x_b. In Fig. 3, the local grid step at the boundary is $\delta x_b = x_b - x_{b-1} = 6 - 5.88$.

The RRM was performed for a variety of initial grids [initialized with different functions $y^{in}(x)$], with different spacing and with various choices of the simplex. Independent of these variations, the RRM iterations converged stably to the analytical SIM of the DS system. Results are presented in Fig. 3 for two different initial grids: a regular linear ($y^{in} = ax$, $a = 0.25$) and a randomly generated grid [for each value
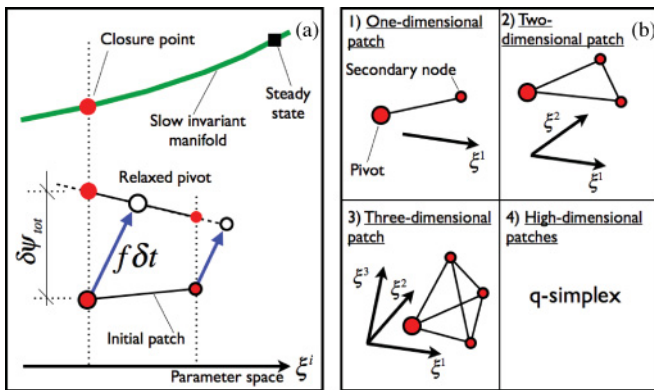

FIG. 4. (Color online) (a) Relaxation redistribution method: Local formulation. Only a small patch of the SIM is constructed. After refinement, the coordinates of the pivot provide the reduced system (17) with a closure. (b) Simplexes can be conveniently adopted for a patchwise description of the SIM in any dimension.

$x_r \in [0,6]$ a random number $y^{in}(x_r) \in]0,1[$ is assigned by a linear congruent generator] with the intervals Σ_1 chosen as $x_1 - x_0 = 0.12$. Convergence to SIM is even striking in Fig. 3 given the fact that both initial grids are far from SIM.

Thus, convergence of the RRM iterations confirms the existence of a reduced description with a fixed number of degrees of freedom q (existence of q-dimensional slow invariant manifold). On the contrary, no convergence in RRM indicates that more degrees of freedom are needed to recover the detailed system dynamics. This concept shall be used below for adaptively choosing the invariant grid dimension.

Both construction and usage of a global reduced description soon become impracticable as the dimension q increases. In fact, computing and storage of high dimensional SIMs may be problematic already at $q \geqslant 3$. Above all that, data retrieval by interpolation on such large arrays is computationally intensive, and sometimes full construction of manifolds can be useless: For example, in combustion applications, regions with a high concentration of radicals are unlikely to be visited.

Remark: In general, when using model reduction techniques, such as the RRM method, slow and fast subspaces are not known in advance. In fact, this kind of information is what we get at the end of the process. Invariant grids constructed by the suggested RRM are finally located in the slow subspace (regardless of the choice on the parametrization). The fast subspace can be thereafter reconstructed by adopting, e.g., the notion of thermodynamic projector (see, e.g., Refs. [15], [16], and [19]). On the other side, concerning the parametrization choice, we notice that (as stressed in Sec. VI) there are no universal recipes, and it specifically depends on the physical phenomenon we are dealing with. In general, good macroscopic variables can be found in the literature: For instance, in the case of the Boltzmann equation, typical macroscopic parameters are the velocity moments of the distribution function, whereas for chemical kinetics we can use spectral variables, as done for the example in Sec. V. Alternatively, in the latter case, typical slow variables can also be adopted [see, e.g., the rate controlled constrained equilibrium (RCCE) parametrization in Ref. [25]].

B. Local formulation of RRM

Importantly, the RRM allows for a straightforward local formulation, where only small patches of the slow invariant grid are initialized and refined (see Fig. 4). Let $\bar{\xi} = (\bar{\xi}^1, \dots, \bar{\xi}^q)$, and the procedure is initialized with a simplex $\bar{S}_q$ where the pivot $\bar{\psi}^{in} = \psi^{in}(\bar{\xi})$ is linked to q secondary nodes $\psi_1^{in} = \psi^{in}(\bar{\xi}_1), \dots, \psi_q^{in} = \psi(\bar{\xi}_q)$ in a neighborhood of $\bar{\psi}$ such that $\bar{\xi}_i = (\bar{\xi}^1, \dots, \bar{\xi}^i + \delta\xi^i, \dots, \bar{\xi}^q)$, with $\delta\xi^i$ being a small deviation of the ith macroscopic variable. A sequence of relaxation and redistribution steps is applied to the vertices of $\bar{S}_q$ in any dimension q: This realizes indeed the simplest instance of the RRM,

$$\bar{\psi}^{RR} = \left(1 - \sum_{i=1}^q w_i\right)\bar{\psi}^R + \sum_{i=1}^q w_i \psi_i^R, \qquad (20)$$

while the weights w_i are found from the redistribution (antishagreen) condition (15): $b(\bar{\psi}^{RR}) = \bar{\xi}$. Refinements end as soon as a norm of the total displacement of the pivot at

the nth RRM iteration, $|\delta\bar{\psi}^{\text{tot}}_{(n)}| = |\bar{\psi}^{\text{RR}}_{(n+1)} - \bar{\psi}^{\text{RR}}_{(n)}|$, becomes sufficiently small compared to the displacement caused by the relaxation alone, $|\delta\bar{\psi}^{\text{rel}}_{(n)}| = |\bar{\psi}^{\text{R}}_{(n+1)} - \bar{\psi}^{\text{R}}_{(n)}|$.

Setting an upper limit to both the number of refinements N and the tolerance ϵ such that

$$\left|\delta\bar{\psi}^{\text{tot}}_{(n)}\right| \Big/ \left|\delta\bar{\psi}^{\text{rel}}_{(n)}\right| \leqslant \epsilon, \tag{21}$$

the local RRM can be adaptively performed starting with $q = 1$. If the latter requirements are not fulfilled, the dimension is updated to $q = 2$ and the procedure repeated. Upon convergence with some $q = \bar{q}$, a closure of the reduced system (17) is provided by the coordinates of the pivot. It is worth stressing that the above convergence criterion (21) is based on the value assigned to the tolerance ϵ and number of refinements N. However, the latter quantities can be properly set upon an independence study with respect to the manifold dimension. Namely, in the same spirit of grid independence studies of fluid dynamics simulation results, the independence of the manifold dimension q on ϵ and N can be verified by repeating the calculations with smaller tolerances and larger number of refinements. In this sense, the local RRM fully alleviates any assumption about the dimensionality of SIM, the local dimension is found automatically, and if no reduced description is possible at all, no convergence at any $q < n$ will clearly indicate this.

Finally, for systems supported by a Lyapunov functions G [such as the kinetic equations (3)], a convenient (but not the only possible) initialization of the RRM procedure (construction of the initial pivot and secondary nodes) for dissipative systems can be accomplished by means of the notion of quasiequilibrium manifold (QEM). In this respect, an approximation of the q-dimensional SIM can be obtained by minimizing the function G under q linear constraints in addition to the element conservation laws (8):

$$\begin{cases} G \to \min, \\ b_i(\psi) = \xi^i, \quad i = 1, \dots, q, \\ C\psi = \text{const}, \end{cases} \tag{22}$$

where, in the case of chemical kinetics, the function G is a thermodynamic potential (i.e., entropy, Gibbs free energy, etc.), as discussed in Sec. II A. It is worth stressing that the idea of using extrema of potentials, for providing a reduced description with a closure, dates back to the work of Gibbs [32]. From then on, this notion has been adopted in several areas, such as the kinetic theory of gases [15,33], or detailed combustion mechanisms [25]. However, we stress that the latter approximations often provide a poor description of the corresponding SIM [27,34], and thus they are used here only for initializing the RRM.

Below, following the suggestion in Ref. [35], we make use of spectral variables $\xi^i = b_i(\psi)$ obtained by the inner product between the state ψ and the parametrization vectors b_i, which are the left eigenvectors of the Jacobian $J = \partial f / \partial \psi$ at the steady state, corresponding to nonzero eigenvalues λ_i and numbered in the order of increase of $|\lambda_i|$. The latter is referred to as spectral quasiequilibrium parametrization. The pivot $\psi^* = (\psi_1, \dots, \psi_n)$ of the initial simplex $\bar{S}_q$ is defined as the quasiequilibrium point [15], corresponding to $\bar{\xi} = (\bar{\xi}^1, \dots, \bar{\xi}^q)$, and calculated by solving the problem (22).

To this end, (22) is equivalent to the global minimization problem of a Lagrange function $\bar{G}$:

$$\bar{G} = G + \sum_{i=1}^{q} [b_i(\psi) - \xi^i]\tilde{\lambda}_i + \tilde{\lambda}C\psi, \tag{23}$$

with $\tilde{\lambda}_i, \tilde{\lambda}$ being a set of Lagrange multipliers. We notice that efficient tools for the solution of (22) are also available (see, e.g., STANJAN [36]). Secondary nodes ψ^k of the simplex can be conveniently calculated by linear expansion of the minimization problem about the quasiequilibrium as suggested in Ref. [34]: $\psi^k = \psi^* + \sum_{i=1}^{n-d} \delta^i_k \rho_i$, with $(\rho_1, \dots \rho_{n-d})$ and $\delta_k = (\delta^1_k, \dots, \delta^{n-d}_k)$ being a vector basis spanning the null space of C and the solution of a linear algebraic system

$$\begin{cases} \sum_{i=1}^{n-d} (t_j H^* \rho_i)\delta_i = -\nabla G^* t_j, \quad j = 1, \dots, n-d-q, \\ \sum_{i=1}^{n-d} (b_1 \rho_i)\delta_i = 0, \\ \dots \\ \sum_{i=1}^{n-d} (b_k \rho_i)\delta_i = \varepsilon_k, \\ \dots \\ \sum_{i=1}^{n-d} (b_q \rho_i)\delta_i = 0. \end{cases} \tag{24}$$

The vector basis $(t_1, \dots t_{n-q-d})$ spans the kernel of the linear space defined by the vectors b_i and the rows of the matrix C in (8), $H^* = [\partial^2 G / \partial\psi_i \partial\psi_j]$ and $\nabla G^* = [\partial G / \partial\psi_i]$ are the second derivative matrix and the gradient of the function G at the pivot, respectively, while ε_k defines the length of the edge of the simplex Σ_q along the kth direction.

V. ILLUSTRATION: DETAILED HYDROGEN-AIR MIXTURE

Here we consider the autoignition of the hydrogen-air mixture at stoichiometric proportion, reacting according to the realistic detailed mechanism of Li *et al.* [3], where nine chemical species and three elements participate in a complex reaction dictated by 21 reversible elementary steps (2) (this mechanism is universally used in turbulent combustion simulations [4], and details for this case are discussed in the Appendix). The time evolution of species concentration is governed by (3), and it is supplemented by the condition for the reactor temperature, which stipulates the conservation of the mixture enthalpy (adiabatic reactor):

$$\bar{h} = \sum_{i=1}^{9} h_i Y_i = 1000 \text{ (kJ/kg)}. \tag{25}$$

Furthermore, the pressure of the mixture is fixed [$p = 1$ (atm)], and the mass fraction (Y_i) of an arbitrary chemical species i can be expressed in terms of the corresponding molar concentration (c_i) by means of the following relationship:

$$Y_i = \frac{c_i \omega_i}{\sum_{j=1}^{n} c_j \omega_j}. \tag{26}$$

Figure 5 shows a projection of the heterogeneous SIM (i.e., with a varying dimension in the phase space), onto the subspace $\xi^1, \xi^2, \xi^3, Y_{\text{OH}}$, constructed by the local RRM, where one-, two-, and three-dimensional patches are clearly visible. Here, the variables ξ^1, ξ^2, ξ^3 are chosen according
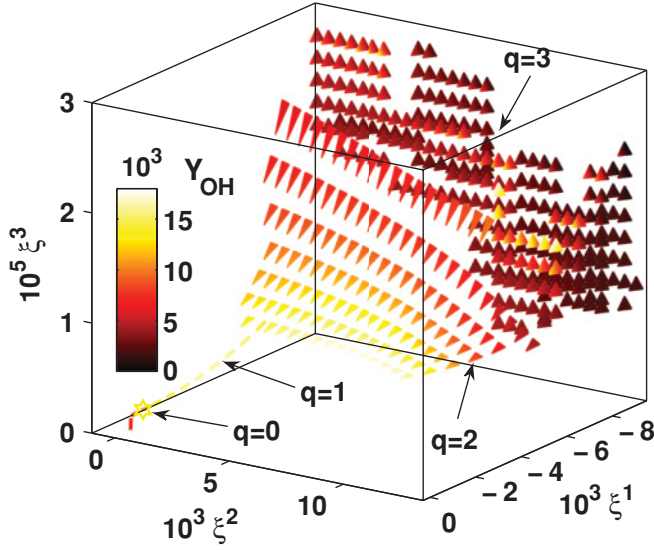
FIG. 5. (Color online) Heterogeneous slow invariant manifold of hydrogen-air combustion mechanism by local RRM. Three-dimensional projection of the six-dimensional phase space onto spectral variables (see text). The two-dimensional patch ("kite", triangles) is tight by a one-dimensional "thread" (line) to the zero-dimensional equilibrium and merges with the three-dimensional "cloud" (tetrahedra). Legend: mass fraction of OH. Explicit Euler scheme with $\delta t = 5 \times 10^{-8}$(s) was used for the relaxation of simplexes. RRM convergence criteria: $N = 2000$, $\epsilon = 10^{-4}$.
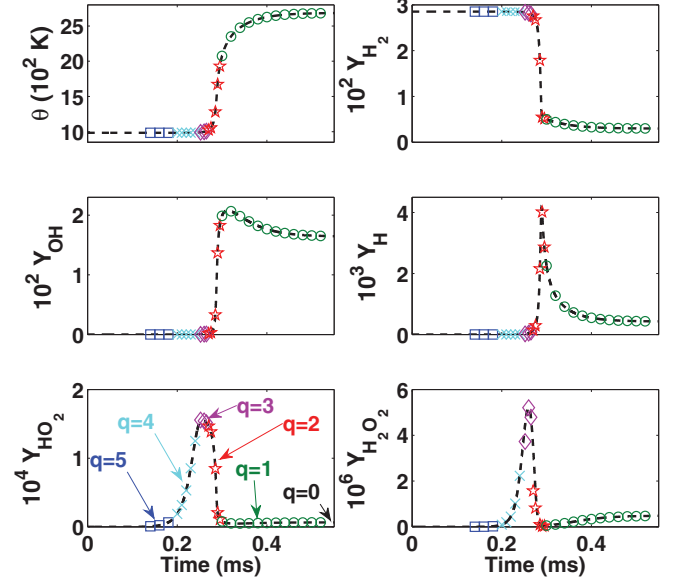

FIG. 6. (Color online) Autoignition of homogeneous stoichiometric mixtures of hydrogen and air: Histories of the temperature and of the mass fraction of chemical species. The line shows the detailed reaction. Symbols show the local RRM method by adaptively following a cascade of reduced models of various dimension q: $q = 5$ (squares), $q = 4$ (crosses), $q = 3$ (diamonds), $q = 2$ (stars), $q = 1$ (circles), and $q = 0$ (steady state).

to the spectral quasiequilibrium parametrization, where $\xi^i = b_i(\psi) = b_i \psi$, with b_i denoting the three slowest eigenvectors of the Jacobian matrix $J = \partial f / \partial \psi$ at the steady state, whereas the RRM is initialized as discussed above in the text with the potential G computed on the basis of the mixture-averaged entropy (9). Interested readers may find full details on the computation of G and its derivatives [∇G and H^* requested in (24)] in Ref. [37]. Results in terms of basic variables (i.e., concentrations of species) can be obtained upon a postprocessing of the spectral variables, which amounts to a linear transformation.

A typical problem, where dynamics evolves along a cascade of slow invariant manifolds with progressively lower dimensions, is the autoignition of a fuel-air mixture. In Fig. 6, the solution of the reduced system (17), supplemented with a closure by the local formulation of RRM, is compared with the integration of the detailed reaction mechanism. Results are in excellent agreement for all the chemical species and the temperature. Note that, although one- and two-dimensional SIMs are able to recover the most of the dynamics of major species and of the temperature, the minority species (such as radicals HO_2 and H_2O_2) do require high-dimensional manifolds ($q \geqslant 3$) to be correctly predicted.

For the sake of clarity, we outline below the steps leading to the computation of a q-dimensional closure corresponding to a macroscopic state $\xi = (\xi^1, \ldots, \xi^q)$, by the local RRM for the above kinetic system:

(1) Set up the initial SIM dimension (e.g., $q = 1$).

(2) Set up a convergence criterion (21), and the maximal number of iterations N.

(3) Compute the initial coordinates of the pivot ψ^*, which amounts to solving a nonlinear algebraic system, $\nabla \tilde{G} = 0$, e.g. by Newton-Raphson iterations.

(4) Compute q secondary nodes ψ^k by the linear algebraic system (24).

(5) Update the coordinates of both the pivot and secondary nodes by the RRM Eq. (20).

(6) Check convergence.

(7) If no convergence is achieved after N iterations, then update the SIM dimension $q = q + 1$ and go to 3.

(8) Exit.

The above illustration demonstrates that the suggested RRM method is able to accurately recover the dynamics of a complex system. Moreover, here we adopted the automatic criterion (21) to choose the number of reduced degrees of freedom (macroscopic important variables), which are strictly needed to reproduce the phenomenon under study. The latter features make the RRM, on one side, a very useful tool for the efficient computation of large dissipative systems. Most importantly, on the other side, it enables to gain a better physical understanding about a complex phenomena by addressing the issue of its minimal description.

VI. CONCLUSION

To conclude, we addressed here the fundamental problem of the minimal description of a complex dissipative system, which is a challenging issue in physics. Our approach is based on a simulation (instead of a solution) of the fundamental film equation of dynamics (11). We stress that it is the RRM realization that is able to unfold the full power of the method

of invariant manifold, which was not possible before, such as the adaptive construction of high-dimensional manifolds (i.e., $q \geqslant 3$, with q varying from a region of the phase space to another). On the practical side, RRM is fairly simple as it is based on a direct integration of the kinetic system plus redistribution. The key point realized in this paper is that the latter simulates subtraction of slow motion from the film dynamics, a step that is hard to control in more conventional approaches to the film equation [19]. In that respect, the RRM is similar in spirit (but certainly not in the implementation) to other successful simulation strategies, such as the direct simulation Monte Carlo method [38], which replaces the solution of the Boltzmann equation by a stochastic simulation of "collisions." We stress that suitable macroscopic variables depend on the specific phenomenon (e.g., velocity moments of the distribution function for describing gas kinetics [22,39]). The methodology developed in this paper addresses the general problem of minimal macroscopic description by letting the system decide how many important variables are to be considered.

Examples presented above convincingly show that RRM achieves all the objectives set for obtaining the accurate reduced description, whereas the resulting adaptively reduced models reveal new physical knowledge of a complex dissipative system (i.e., its minimal description), which can be used for its computationally efficient simulation. We should stress that fully adaptive construction of heterogeneous slow invariant manifolds as in the case of a hydrogen-air mixture is difficult if at all possible with any other model reduction technique [7]. Finally, while we focused on the important class of dissipative systems arising in combustion, we look forward to a generalization of the above technique of simplification to other dissipative systems such as master and Fokker-Planck equations and other complex dynamics.

APPENDIX: DETAILED REACTION FOR HYDROGEN AND AIR

In Table I, we list all reaction steps involved in the combustion mechanism for hydrogen and air adopted in Sec. V, where $n = 9$ species (H_2, N_2, H, O, OH, O_2, H_2O, HO_2, H_2O_2) and $d = 3$ elements (H, O, N) are involved in $r = 21$ elementary reversible steps. The system of kinetic equations is formulated according to (3) and (4), where the reaction constant k_s^+ of the sth step is determined by the Arrhenius law (5) with the coefficients A_s, n_s, and Ea_s from Table I. In the following, the symbol M represents an additional species, whose concentration c_M denotes a weighted sum of

TABLE I. Detailed H_2-air reaction mechanism. Units are cm³, mol, s, Kcal, and K.

Reaction		A_s	n_s	Ea_s
1. $H + O_2 \rightleftharpoons O + OH$		3.55×10^{15}	-0.41	16.6
2. $O + H_2 \rightleftharpoons H + OH$		5.08×10^4	2.67	6.29
3. $H_2 + OH \rightleftharpoons H_2O + H$		2.16×10^8	1.51	3.43
4. $O + H_2O \rightleftharpoons OH + OH$		2.97×10^6	2.02	13.4
5. $H_2 + M \rightleftharpoons H + H + M$		4.58×10^{19}	-1.40	104.38
6. $O + O + M \rightleftharpoons O_2 + M$		6.16×10^{15}	-0.50	0.00
7. $O + H + M \rightleftharpoons OH + M$		4.71×10^{18}	-1.0	0.00
8. $H + OH + M \rightleftharpoons H_2O + M$		3.8×10^{22}	-2.00	0.00
9. $H + O_2(+M) \rightleftharpoons HO_2(+M)$[a]	k_0^+	6.37×10^{20}	-1.72	0.52
	k_∞^+	1.48×10^{12}	0.60	0.00
10. $HO_2 + H \rightleftharpoons H_2 + O_2$		1.66×10^{13}	0.00	0.82
11. $HO_2 + H \rightleftharpoons OH + OH$		7.08×10^{13}	0.00	0.30
12. $HO_2 + O \rightleftharpoons O_2 + OH$		3.25×10^{13}	0.00	0.00
13. $HO_2 + OH \rightleftharpoons H_2O + O_2$		2.89×10^{13}	0.00	-0.50
14. $HO_2 + HO_2 \rightleftharpoons H_2O_2 + O_2$		4.20×10^{14}	0.00	11.98
15. $HO_2 + HO_2 \rightleftharpoons H_2O_2 + O_2$		1.30×10^{11}	0.00	-1.63
16. $H_2O_2(+M) \rightleftharpoons 2OH(+M)$[b]	k_0^+	1.20×10^{17}	0.00	45.5
	k_∞^+	2.95×10^{14}	0.00	48.4
17. $H_2O_2 + H \rightleftharpoons H_2O + OH$		2.41×10^{13}	0.00	3.97
18. $H_2O_2 + H \rightleftharpoons HO_2 + H_2$		4.82×10^{13}	0.00	7.95
19. $H_2O_2 + O \rightleftharpoons OH + HO_2$		9.55×10^6	2.00	3.97
20. $H_2O_2 + OH \rightleftharpoons HO_2 + H_2O$		1.00×10^{12}	0.00	0.00
21. $H_2O_2 + OH \rightleftharpoons HO_2 + H_2O$		5.8×10^{14}	0.00	9.56

[a]Troe parameter is 0.8.
[b]Troe parameter is 0.5.

the concentration of all species (third-body reaction):

$$c_M = \sum_{i=1}^{n} a_i c_i, \tag{A1}$$

a_i being the third-body efficiencies. In reactions No. 5–8 shown in Table I, it is adopted $a_{H_2O} = 11.0$, $a_{H_2} = 1.5$, and $a_i = 1$ for all other species. Finally, steps No. 9 and No. 16 are typical falloff reactions, where the reaction constant k_s^+ remarkably depends on the mixture pressure. In this case, k_∞^+ and k_0^+ are the reaction constants in the high- and low-pressure limit, respectively, and the reaction constant reads

$$k_s^+ = k_\infty^+ F P_r / (1 + P_r), \tag{A2}$$

with $P_r = k_0^+ c_M / k_\infty^+$, and F given by the Troe function (see Ref. [40] for the details). In particular, in reaction step No. 9 the third-body efficiencies are $a_{H_2O} = 10$, $a_{O_2} = -0.22$, and in reaction step No. 16, $a_{H_2O} = 11$, $a_{H_2} = 1.5$, whereas in both cases $a_i = 1$ for the rest of the species.

[1] N. Jamshidi and B. Ø. Palsson, Mol. Syst. Biol. **4**, 171 (2008).

[2] D. Endy and R. Brent, Nature (London) **409**, 391 (2001).

[3] J. Li, Z. Zhao, A. Kazakov, and F. L. Dryer, Int. J. Chem. Kinet. **36**, 566 (2004).

[4] "Nur eine kleine Flamme und schon so kompliziert," Interview with Prof. K. Boulouchos, NZZ Neue Zürcher Zeitung (July 05, 2009).

[5] G. Pizza, C. E. Frouzakis, J. Mantzaras, A. G. Tomboulides, and K. Boulouchos, J. Fluid Mech. **658**, 463 (2010).

[6] D. Goussis and U. Maas, in *Turbulent Combustion Modeling*, edited by T. Echekki and E. Mastorakos (Springer, Berlin, 2011), pp. 193–220.

[7] *Model Reduction and Coarse-graining Approaches for Multiscale Phenomena*, edited by A. N. Gorban, N. Kazantzis, I. G.

Kevrekidis, H. C. Öttinger, and C. Theodoropoulos (Springer, Berlin, 2006).

[8] U. Maas and S. B. Pope, Combust. Flame **88**, 239 (1992).

[9] S. H. Lam and D. A. Goussis, Int. J. Chem. Kin. **26**, 461 (1994).

[10] V. Reinhardt, M. Winckler, and D. Lebiedz, J. Phys. Chem. A **112**, 1712 (2008).

[11] H. C. Öttinger, Phys. Rev. Lett. **104**, 120601 (2010).

[12] C. A. Truesdell, *Six Lectures on Modern Natural Physics* (Springer, Berlin, 1966).

[13] P. Asinari, Comput. Phys. Commun. **181**, 1776 (2010).

[14] R. Kee, G. Dixon-Lewis, J. Warnatz, M. Coltrin, and J. Miller, "A Fortran computer code package for the evaluation of gas-phase multicomponent transport properties, Report No. SAND86-8246, Sandia National Laboratories," (1996).

[15] A. N. Gorban and I. V. Karlin, *Invariant Manifolds for Physical and Chemical Kinetics* (Springer, Berlin, 2005).

[16] E. Chiavazzo, I. V. Karlin, and A. N. Gorban, Commun. Comput. Phys. **8**, 701 (2010).

[17] A. G. Ramm, J. Math. Phys. **50**, 042701 (2009).

[18] A. N. Gorban and I. V. Karlin, Chem. Eng. Sci. **58**, 4751 (2003).

[19] A. N. Gorban, I. V. Karlin, and A. Y. Zinovyev, Physica A **333**, 106 (2004).

[20] J. Nafe and U. Maas, Combust. Theory Modell. **6**, 697 (2002).

[21] R. Courant, K. O. Friedrichs, and H. Lewy, IBM J. **11**, 215 (1967).

[22] I. Müller and T. Ruggeri, *Rational Extended Thermodynamics* (Springer, New York, 1998).

[23] I. V. Karlin, M. Colangeli, and M. Kröger, Phys. Rev. Lett. **100**, 214503 (2008).

[24] H. Struchtrup, *Macroscopic Transport Equations for Rarefied Gas Flows* (Springer, Berlin, 2005).

[25] J. C. Keck and D. Gillespie, Combust. Flame **17**, 237 (1971).

[26] D. Lebiedz, J. Chem. Phys. **120**, 6890 (2004).

[27] Z. Ren, S. B. Pope, A. Vladimirsky, and J. M. Guckenheimer, J. Chem. Phys. **124**, 114111 (2006).

[28] H. de Balzac, *La Peau de chagrin* (1831).

[29] E. Chiavazzo, Ph.D. thesis, Swiss Federal Institute of Technology, ETH-Zurich, 2009.

[30] S. B. Pope, Combust. Theory Modell. **1**, 41 (1997).

[31] M. J. Davis and R. T. Skodje, J. Chem. Phys. **111**, 859 (1999).

[32] G. W. Gibbs, *Elementary Principles of Statistical Mechanics* (Dover, New York, 1960).

[33] M. N. Kogan, *Rarefied Gas Dynamics* (Plenum, New York, 1969).

[34] E. Chiavazzo and I. V. Karlin, J. Comput. Phys. **227**, 5535 (2008).

[35] E. Chiavazzo, A. N. Gorban, and I. V. Karlin, Commun. Comput. Phys. **2**, 964 (2007).

[36] W. C. Reynolds, "The element potential method for chemical equilibrium analysis: implementation in the interactive program STANJAN" Mechanical Engineering Department Report, Stanford University," 1986.

[37] E. Chiavazzo, I. V. Karlin, A. N. Gorban, and K. Boulouchos, Combust. Flame **157**, 1833 (2010).

[38] G. A. Bird, *Molecular Gas Dynamics and the Direct Simulation of Gas Flows* (Clarendon, Oxford, 1994).

[39] H. Grad, Commun. Pure Appl. Math. **2**, 325 (1949).

[40] C. K. Law, *Combustion Physics* (Cambridge University Press, Cambridge, UK, 2006).